FAST TRACK COMMUNICATION

Single-sided device for magnetic particle imaging

Timo F Sattel[1]**, Tobias Knopp**[1]**, Sven Biederer**[1]**, Bernhard Gleich**[2]**,**
Juergen Weizenecker[2]**, Joern Borgert**[2] **and Thorsten M Buzug**[1]

[1] Institute of Medical Engineering, University of Lübeck, 23538 Lübeck, Germany
[2] Philips Technologie GmbH Forschungslaboratorien, 22335 Hamburg, Germany

E-mail: sattel@imt.uni-luebeck.de

Abstract
Recently, a new imaging modality called magnetic particle imaging (MPI) was introduced.
The method is capable of imaging the distribution of superparamagnetic nanoparticles at high
sensitivity, high resolution and high imaging speed by exploiting their non-linear
magnetization curve. Up to now, all published simulation as well as experimental work uses a
scanner setup, where the field of view (FOV) lies in between a symmetric coil configuration.
This, however, poses a size limitation for the specimens. In this paper, we present a feasibility
study of a new, so-called *single-sided* scanner, which is applied to the object of interest merely
from one side. Thus, the problem of the specimen fitting into the scanner no longer exists,
which denotes a major step for MPI. To date, the FOV of the single-sided device is limited to
one dimension. First experimental results on imaging phantoms containing a
superparamagnetic fluid show a resolution of up to 1 mm and are indeed promising.

1. Introduction

Using magnetic particle imaging (MPI), one can measure the spatial distribution of magnetic nanoparticles at high sensitivity, high resolution and high imaging speed. It exploits the nonlinearity of the superparamagnetic iron oxide (SPIO) nanoparticle magnetization curve, described by the Langevin theory of paramagnetism [1]:

$$\vec{M}(\vec{r}, t) = M_0(\vec{r}) \left[\coth\left(\frac{m|\vec{B}(\vec{r}, t)|}{(k_B T)} \right) - \frac{(k_B T)}{m|\vec{B}(\vec{r}, t)|} \right] \vec{e}_{\vec{B}}(\vec{r}, t).$$
(1)

Here, $\vec{B}(\vec{r}, t)$ denotes the magnetic flux density at position $\vec{r}$ and time t. The saturation magnetization $M_0(\vec{r}) = c(\vec{r})m$ comprises the concentration of particles $c(\vec{r})$ and the magnetic moment of a nanoparticle $m = \frac{1}{6}\pi D^3 M_S$, which in turn is given by the particle diameter D and the saturation magnetization $M_S = 477\,\text{kA}\,\text{m}^{-1}$ of magnetite (Fe_3O_4) [2].

In order to image the spatial nanoparticle distribution, a magnetic selection field that provides a field free point (FFP)

and a superimposed magnetic drive field are applied. The former ensures spatial encoding, while the latter changes the nanoparticle magnetization. This temporal change induces a signal in one or several recording coils exploited for image reconstruction.

To date, MPI scanner designs consist of at least one coil pair for each encoding dimension [3, 4] with the scannable field of view (FOV) situated in between this coil assembly. Such a setup is shown in figure 1, further referred to as the *conventional* design. Due to the required field strengths, the first scanner was designed such that it only fits small specimens [5]. Even though simulations show that, in principle, whole-body human scanners are feasible [6], they have not yet been realized and scaling up requires further development.

In their original paper [3] in 2005, Gleich and Weizenecker conjectured that a *single-sided* scanner design could work in practice. Here, all coils to generate the required magnetic fields and to receive the nanoparticle response are positioned to one side of the object of interest. Although the depth of penetration, from where information about the nanoparticle distribution can be obtained, is limited, the total object size is

J. Phys. D: Appl. Phys. **42** (2009) 022001

IOP FTC ▶▶▶

Fast Track Communication
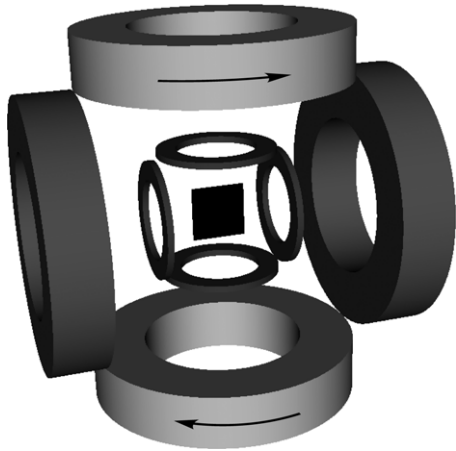
Figure 1. Setup of a conventional MPI scanner for 2D imaging [5] consisting of two pairs of transmit coils and two pairs of smaller receive coils. The selection field is generated by direct currents of opposite direction (indicated by arrows). The 2D FOV is situated in between the coil setup indicated schematically as a black rectangle.

no longer of relevance. This is an essential advantage, which is also provided by other tomographic imaging modalities, as for instance ultrasound, optical coherence tomography or single-sided nuclear magnetic resonance imaging [7].

2. Theory

A reasonable single-sided device to achieve an FFP suitable for MPI is shown in figure 2, where two transmit coils are situated concentrically. When a direct current of opposite direction is applied to each coil, their generated magnetic fields superimpose such that they cancel out in two points. Due to the rotational symmetry of the configuration, these FFPs are situated on the coil axis, one on either side of the setup (figure 3). Since the scanner is applied to the object from one side, one of the FFPs enters the object. The other one remains inside the scanner device and therefore cannot be exploited for imaging. Correspondingly, it is not necessary to further consider this point when it is ensured that no magnetic material is applied inside the scanner.

In addition to the time-invariant selection field, a time-dependent drive field is generated. This can be achieved by applying an additional ac current to one or both of the transmit coils. Consequently, the FFP moves on a 1D trajectory along the x-axis, which coincides with the coil axes. Depending on the strength of the selection field and the amplitude of the drive field, a 1D FOV of several centimetres length can be achieved.

Due to saturation effects, the nanoparticle response evoked by the movement of the FFP consists not only of the drive field frequency f_0 but also of higher harmonics. In MPI, this signal is used for reconstructing the spatial distribution of nanoparticles. To measure the nanoparticle response, a receive coil is required, which in general may be the same as one of the transmit coils. The receive signal can then be separated from the transmit signal by an analog filter.

As derived in [3] and confirmed in [5], the spatial resolution depends on the gradient G of the selection field.
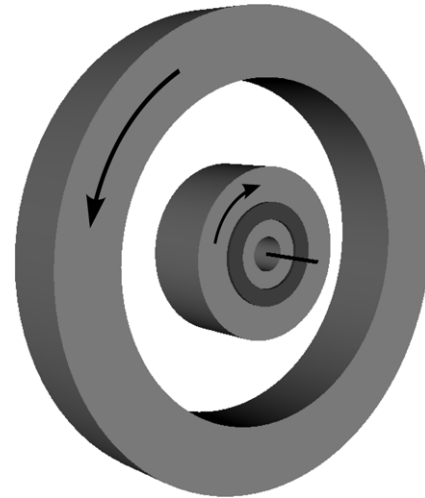
Figure 2. Setup of a single-sided MPI scanner made up of two concentrically positioned transmit coils (light grey) and a separate receive coil (dark grey). The selection field is generated by direct currents of opposite direction (indicated by arrows). The 1D FOV is indicated schematically as a black line.
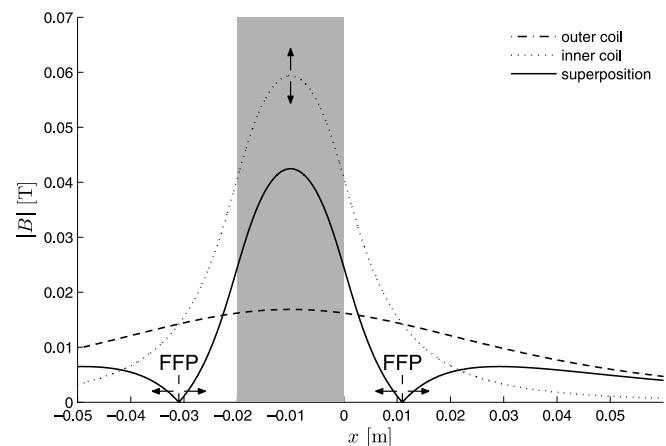
Figure 3. Resulting magnetic flux density $B(x)$ (absolute values) of the selection field along the coil axis. Two FFPs are present, one on each side of the coils of which the position is indicated by the grey background. The effect of FFP movement (indicated by arrows) is caused by an additional drive field current applied to the inner coil.

In the conventional scanner design, G is almost homogeneous within the FOV. Hence, the resolution can be assumed to be spatially independent. Here, the resolution is expected to be high in the vicinity of the scanner and to decrease with increasing distance. This is in accordance with the highly inhomogeneous gradient field of the single-sided setup.

Furthermore, the receive coil is applied only from one side. Since its sensitivity profile is highly inhomogeneous, the signal-to-noise ratio (SNR) is spatially dependent as well. This in turn will further lower the imaging quality for objects far from the scanner.

3. Materials and methods

To prove the feasibility of the introduced single-sided scanner concept, a prototype is manufactured. The two transmit coils

J. Phys. D: Appl. Phys. **42** (2009) 022001

IOP FTC ▶▶▶

Fast Track Communication

consist of 36 windings, each of which has a length of 20 mm, a width of 20 mm and an outer diameter of 50 mm and 140 mm, respectively. At present, the receive coil is set up separately. This allows for testing different receive coil configurations having distinct sensitivity profiles. In this paper, the flat spiral receive coil is made up of 15 windings resulting in an inner diameter of 19 mm and an outer diameter of 39 mm. It is directly mounted concentrically on the inner transmit coil.

To generate the selection field, a direct current of $I_S = 43$ A is applied to the transmit coils in opposite directions. As long as no additional drive field is applied, the FFP is located at $x = 10.97$ mm in front of the transmit coils. When the drive field, generated by an alternating current of amplitude $I_S = 48$ A and frequency $f_0 = 25$ kHz, is superimposed on the inner transmit coil, the FFP moves on the x-axis to about $x = 20$ mm for positive superposition and vanishes at $x = -10$ mm for negative superposition. Note that the drive field excitation is sinusoidal but the FFP position $x(t)$ is non-sinusoidal due to the inhomogeneous field geometry.

The transmit path consists of a computer, controlling the dc source (SM 15-200 D, Delta Elektronika BV) and generating the ac signal on a data acquisition card (SMT8036E, Sundance Multiprocessor Technology Ltd), and a power amplifier (DCU2250-28, MT MedTechEngineering GmbH). The inner transmit coil, on which the ac signal is superimposed to the dc current, is connected in series with a capacitor such that it operates at resonance at frequency f_0. This circuit is matched to the power amplifier by a capacitive voltage divider. To protect the dc source against the ac current, the outer transmit coil is part of a passive notch filter rejecting power at f_0.

The change in nanoparticle magnetization induces a signal in the receive coil. Since the transmit coils couple directly to the receive coil, the transmit signal itself is induced as well. Thus, the strong excitation signal is superimposed to the nanoparticle response, which is several orders of magnitude lower. A multi-stage analog filter is necessary to suppress the receive signal at f_0 to allow for an amplification with a low-noise amplifier and digitization. Here, the same data acquisition card as for transmit signal generation is used.

Reconstruction of a 1D image is done by solving the linear system of equations written in matrix vector notation:

$$S\vec{c} = \vec{u}, \qquad (2)$$

where S is the system matrix that maps the vector of received frequency components $\vec{u}$ to the vector of particle concentrations $\vec{c}$. Basically, the method described in [6] is followed. However, instead of performing the direct singular value decomposition method, the iterative Kaczmarz's method [8] is applied. This allows one to consider the physically reasonable constraint that the particle distribution is real positive. It is enforced by setting imaginary and negative values to zero in each iteration cycle.

In order to obtain the system matrix S, a 1-hole phantom is used as a delta-like probe. The hole is drilled in a block of acrylic glass and is 1.0 mm in diameter. With a length of 6 mm, it contains about 4.7 μL undiluted (500 mmol (Fe) L^{-1}) Resovist (Schering AG), which is primarily used as a contrast agent in magnetic resonance imaging. The delta probe is
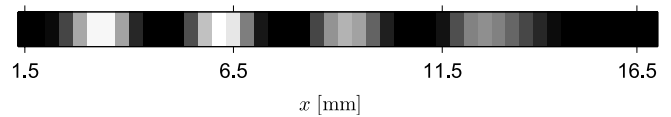
Figure 4. Reconstructed 1D image of the 5-hole phantom (1 mm diameter, 2 mm gap).

shifted to 46 equally spaced positions along a distance of 15 mm covering the FOV while acquiring the induced signal at each sample position. The acquisition time at each position is 6400 drive field periods or 256 ms to achieve a high SNR. The delta probe is moved using a robot (Iselautomation GmbH and Co. KG).

The imaged phantoms consist of two or five aligned holes (diameter 1.0 mm, length 6 mm) filled with undiluted Resovist. To determine the imaging quality of the presented system, these phantoms were imaged at different positions. For each acquired image, the total acquisition time is 51.2 ms equivalent to 1280 drive field periods.

4. Results

In figure 4, a reconstructed 1D image of the 5-hole phantom is shown. It is evident that only four out of the five holes are recovered in the image, which is a direct consequence of the limited FOV. The scanner device is applied from the left, as for all following images. The fifth hole lies just outside the FOV at the right-hand side. Thus, it is not present on the reconstructed image.

Another way to investigate the imaging properties of the presented system is to move a 2-hole phantom away from the scanner setup. The image sequences for a gap of 4 mm and for a gap of 1 mm between the holes are shown in figures 5 and 6, respectively. First, the distance between the scanner front and the first hole filled with superparamagnetic material is 1.83 mm and is increased consecutively by $\frac{1}{3}$ to 14.83 mm in total. With increasing distance from the scanner head, the hole is imaged more blurry and disappears at about $x = 15$ mm. In the sequence with the larger gap, the two holes can clearly be separated at any position, whereas in the other sequence, the holes with the small gap in between can only be separated when placed near the scanner front. With increasing distance, the holes get blurred on the image and can no longer be distinguished. This clearly shows the aforementioned spatial dependence of the resolution of the system.

Since the scanning time for each 1D image is 51.2 ms, and the computation time needed for reconstruction is negligible for 1D images, the scanner can be used online with a repetition rate of almost 20 frames s^{-1}.

5. Discussion

As stated above, the resolution is spatially dependent due to an inhomogeneous field gradient strength G. Near the transmit coils, resolution is about 1 mm due to the high gradient. With increasing distance, G and therefore resolution decreases. Furthermore, it is no longer reasonable to define the FOV only by the trajectory on which the FFP moves along. First, it may

J. Phys. D: Appl. Phys. **42** (2009) 022001

Fast Track Communication
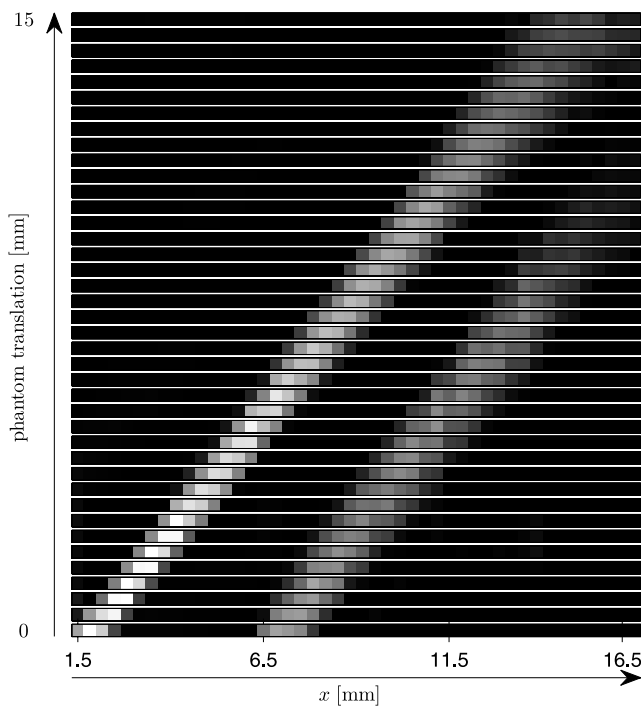
Figure 5. Sequence of reconstructed 1D images of a 2-hole (1 mm diameter, gap 4 mm) phantom. The phantom position x increases consecutively by 0.333 mm.
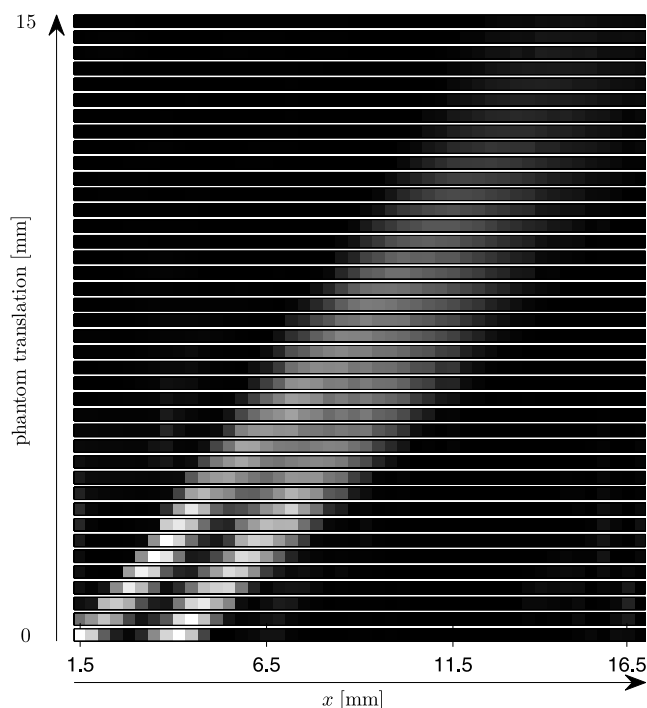
Figure 6. Sequence of reconstructed 1D images of a 2-hole (1 mm diameter, gap 1 mm) phantom. The phantom position x increases consecutively by 0.333 mm.

vanish inside the coil setup. Second, the gradient as well as the sensitivity profile may be too low in the outer regions to achieve a reasonable SNR. Thus, one should further consider criteria affecting the FOV serviceable for imaging. By visual inspection of figures 4 and 5, one may give a resulting FOV of $x = 1.5$–15 mm.

A limited FOV poses a problem to some tomographic imaging methods. In x-ray computed tomography, for example, a complete slice of an object has to be scanned even if only a limited FOV is of interest. Otherwise, missing data about the region outside the FOV cause so-called truncation artifacts on the reconstructed image. Figure 4 shows that this is not the case in MPI. Here, nanoparticles outside the FOV stay almost in saturation. Therefore, their contribution to the receive signal is negligible and does not affect the reconstruction process of the nanoparticle concentration inside the FOV.

The limitations in resolution, contrast, sensitivity as well as in size of the FOV of the present imaging device are a direct consequence of the coil geometry and the limited applied current amplitudes, which in turn are limited by heating. Thus, it is advisable to supply the transmit coils with an improved cooling system, which allows the desired current amplitudes to be increased. Another way is to use strong permanent magnets to generate the selection field. Consequently, the dc current amplitude can be reduced resulting in a lower thermal load as well. One may also think of pulsed scanning patterns to avoid thermal peaks. This might be advisable for small hand-held designs or in material testing where the total scanning time is uncritical.

With the given setup, the FOV is restricted to one dimension. However, similarly to the conventional MPI scanner design, the single-sided setup can be extended by additional transmit coils to achieve a 2D or even a 3D imaging system. It is reasonable to arrange such an additional coil orthogonally to the two transmit coils of the 1D system. Moreover, a setup is possible which consists of at least three coils, which may also be situated in the same plane. However, designing a setup such that the FFP moves along an appropriate multidimensional trajectory is a demanding task.

6. Conclusion

We have demonstrated first experimental results for single-sided MPI. To evaluate the imaging properties, different phantoms are used. As expected, the resolution and contrast decrease with distance from the scanner device. Nevertheless, the presented results are promising. First feasibility could be shown for a new concept for an MPI scanner, which fundamentally differs from existing setups. The potential applications in medicine or material testing of a single-sided MPI scanner differ from prospective whole-body and whole-object scanners, respectively. Due to its nature, the single-sided setup aims at imaging near-surface structures up to a depth of about several centimetres.

References

[1] Chikazumi S and Charap S H 1964 *Physics of Magnetism* (New York: Wiley)
[2] Landolt H and Börnstein R (ed) 1977 *Numerical Data and Functional Relationships in Science and Technology* (*Magnetic Oxides and Related Compounds* vol III/4b) (Berlin: Springer)

J. Phys. D: Appl. Phys. **42** (2009) 022001

IOP FTC ▶▶▶

Fast Track Communication

[3] Gleich B and Weizenecker J 2005 Tomographic imaging using the nonlinear response of magnetic particles *Nature* **435** 1214–7

[4] Weizenecker J, Gleich B and Borgert J 2008 Magnetic particle imaging using a field free line *J. Phys. D: Appl. Phys.* **41** 105009

[5] Gleich B, Weizenecker J and Borgert J 2008 Experimental results on fast 2D-encoded magnetic particle imaging *Phys. Med. Biol.* **53** N81–4

[6] Weizenecker J, Borgert J and Gleich B 2007 A simulation study on the resolution and sensitivity of magnetic particle imaging *Phys. Med. Biol.* **52** 6363–74

[7] Eidmann G, Savelsberg R, Blumler P and Blumich B 1996 The NMR MOUSE, a mobile universal surface explorer *J. Magn. Reson. Ser.* A **122** 104–9

[8] Kaczmarz S 1937 Angenäherte Auflösung von Systemen linearer Gleichungen *Bull. Int. Acad. Pol. Sci. Lett.* A **1937** 355–7